Reviewed research article

Grain characteristics of silicic Katla tephra layers indicate a fairly stable eruption environment between 2800 and 8100 years ago

Edda Sóley Þorsteinsdóttir*, Guðrún Larsen and Esther Ruth Guðmundsdóttir

Institute of Earth Sciences, University of Iceland, Sturlugata 7, 101 Reykjavík, Iceland

**Corresponding author, eddas@mannvit.is*

Abstract — *Grain size and shape analyses were performed on silicic to intermediate Katla tephra (SILK) formed 2800–8100 years ago to examine whether the grain characteristics had changed with time, and in such a case, could they reflect changes in the eruption environment and/or changes in chemical composition. No systematic changes with time were observed in the grain shape parameters (elongation, ruggedness and circularity), however, the second oldest tephra layer SILK-A11 does not have the typical elongated grain shape that characterizes the other SILK tephra layers. Chemical analyses indicate that the SILK layers can be divided into three subgroups but no correlation between chemical composition and the grain parameters is observed. Changes in grain size of the SILK tephra layers with time indicate an apparent increase in grain size occurring about 6000 years ago, where largest grains are of category -3 Φ compared to 0 Φ in the older layers, all sampled at similar distance from source. This change in grain size could result from variation in ice thickness in the Katla caldera, with finer grain size between 6000–8200 years ago being due to thicker ice cover and greater availability of meltwater for magma fragmentation. Conversely, the younger coarser grained SILK layers may have formed under a thinner ice cover. A shift of the eruption sites to an area with thinner ice is also a possibility. However, no radical changes in the eruption environment 2800–8100 years ago are demonstrated by variations in grain characteristics, a conclusion further supported by large jökulhlaups from Mýrdalsjökull ice cap during this period.*

INTRODUCTION

It has been postulated that ice caps and glaciers in Iceland receded dramatically or even disappeared during the Holocene climate optimum (e.g. Björnsson, 2008; Flowers *et al.*, 2008). Óladóttir *et al.* (2007) argued that the Mýrdalsjökull ice cap (Figure 1) has been present for at least 8400 years, based on sulphur content of basaltic Katla tephra that indicates arrested degassing of the erupting magma by quenching in meltwater. Dugmore (1989) dated the outermost moraines of Sólheimajökull outlet glacier to be over 3300 years old (3100 ^{14}C years BP), indicating a large ice cap at that time. According to model calculations presented by Björnsson (2008), the Mýrdalsjökull ice cap did not exist 4000 years ago, but Björnsson assumes that a caldera lake was present during the ice-free period. However, 11 volcanogenic jökulhlaups from the Mýrdalsjökull massif carrying volcanic ash and pumice westwards into Markarfljót are known throughout the 8400 year period (Larsen *et al.*, 2005; Gröndal *et al.*, 2005; Smith and Dugmore, 2006; Eggertsson, 2013). At least eight of the west-going jökulhlaups, dated between 7500 and 1200 years ago, emanated from the caldera via Entujökull, and the two largest ones, ~4400 and ~3500 years ago, had peak discharge of about 200,000 m^3 s^{-1} (Gröndal *et al.*, 2005). This high peak discharge is better explained by a sudden meltwater input than by rapid volume increase in a caldera lake. Deposits of pre-settlement (pre-870 CE) jökulhlaups towards south and east are, however, poorly, or inaccessible, in surface sections and only a few pre-settlement jökulhlaups have been documented (Dugmore, 1989; Maizels, 1994; Larsen, 2010).

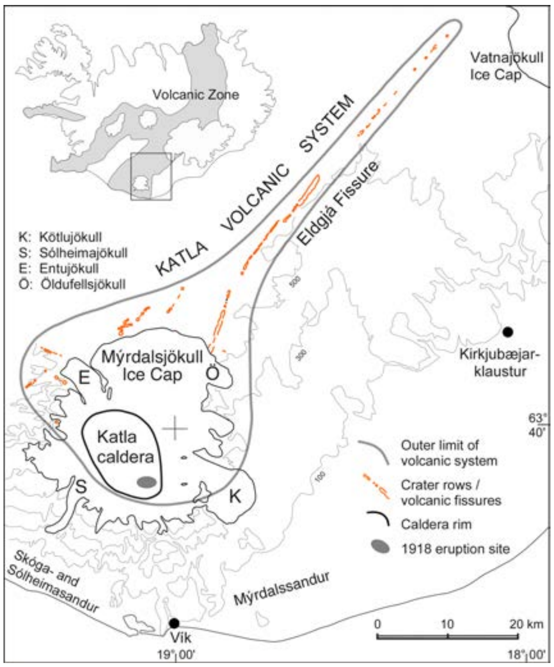

Figure 1. The Katla volcanic system (Larsen, 2000). – *Eldstöðvakerfi Kötlu (Larsen, 2000).*

Grain size and grain morphology can provide important information about an eruption because different eruption conditions influence both size and shape of the grains. Both can help to decide whether the grains are a product of fragmentation by hydromagmatic activity or due to exsolution of magmatic gases (e.g. Sparks *et al.*, 1981; Eiríksson and Wigum, 1989; Dellino and Volpe, 1995, 1996; Dellino and Liotino, 2002; Büttner *et al.*, 2002; Bonadonna and Haughton, 2005; Rose and Durant, 2009; Cioni *et al.*, 2014). These parameters have been studied in individual basaltic and silicic tephra layers (Guðmundsdóttir, 1998; Óladóttir, 2003; Thorsteinsdóttir, 2012; Thorsteinsdóttir *et al.*, 2015), but no systematic investigation of tephra from one volcano, covering an extended period of time has been done until a small pilot study was carried out as a part of a masters project (Thorsteinsdóttir, 2015). Here we investigate whether changes in the grain characteristics of the silicic Katla tephra layers erupted between 2800 and 8100 years ago (Table 1) could throw some further light on the conditions at the volcanic vents and potential changes of the environment during this period.

The Katla volcanic system

The partly ice-covered Katla volcanic system is located in the southern part of the Eastern Volcanic Zone, and is one of the most active Holocene systems in Iceland (Larsen, 2000, 2010; Björnsson *et al.*, 2000; Óladóttir *et al.*, 2005, 2008; Thordarson and Höskuldsson, 2008). It is about 80 km long, trending southwest-northeast (Figure 1), and consists of a central volcano to the southwest, largely covered by the 600 km^2 Mýrdalsjökull ice cap, and a fissure swarm located mostly outside and to the northeast of the glacier. The central volcano has an ice-filled caldera, about 100 km^2 and 700 m deep (Jakobsson, 1979; Björnsson *et al.*, 2000; Larsen, 2000, 2010; Óladóttir *et al.*, 2005, 2008).

Holocene volcanic activity within Katla volcanic system has been divided into three categories:

1. Explosive hydromagmatic/phreatomagmatic basaltic eruptions from short volcanic fissures below the Mýrdalsjökull ice cap are the most frequent type of Katla eruptions and mostly take place within the Mýrdalsjökull caldera.
2. Explosive silicic eruptions are the second most common type during the Holocene. These eruptions originate from vents beneath the ice cap, either inside the caldera or on the caldera fracture and are generally less voluminous than the basaltic eruptions.
3. Effusive basaltic eruptions are less common, occurring outside the glacier along the margins of the central volcano or on the fissure swarm to the northeast, where the two most voluminous eruptions occurred. Where fissures extend under the ice the eruptions are partly explosive.

The eruption history of Katla during the last ∼8400 years is fairly well known, especially the basaltic eruptions. The majority of both basaltic and silicic eruptions begin below the ice cap. In this paper, the focus is on the explosive silicic eruptions.

Table 1. Known silicic Katla tephra layers erupted in the last 8100 years. – *Þekkt súr Kötlu gjóskulög frá síðustu 8100 árum.*

SILK Tephra	^{14}C age BP	^{14}C yrs cal b2k and SAR age	Rounded age	References
YN	1676±12	1622±40	∼1600	Dugmore *et al.*, 2000
UN	2660±50	2850±70	∼2800	Larsen *et al.*, 2001
MN	2975±12	3230±30	∼3200	Larsen *et al.*, 2001
LN	3139±40	3440±75	∼3400	Larsen *et al.*, 2001
N4		∼3920	∼3900	Estimated after Óladóttir *et al.*, 2008
N3		∼4050	∼4100	G. Larsen unpublished data
N2		∼4960	∼5000	After Óladóttir *et al.*, 2005, Table 1b
N1*		∼5830	∼5800	After Óladóttir *et al.*, 2005, Table 1b
A1*		∼6010	∼6000	After Óladóttir *et al.*, 2005, Table 1b
A2		∼6700	∼6700	Estimated after Óladóttir *et al.*, 2005, 2008
A3		∼6900	∼6900	Estimated after Óladóttir *et al.*, 2005, 2008
A5		∼7100	∼7100	Directly above Hekla-5, 7125 cal b2k
A7		∼7180	∼7200	Estimated after Óladóttir *et al.*, 2008
A8		∼7400	∼7400	Estimated after Óladóttir *et al.*, 2008
A9		∼7500	∼7500	Estimated after Óladóttir *et al.*, 2008
A11		∼8000	∼8000	Estimated after Óladóttir *et al.*, 2008
A12		∼8100	∼8100	Estimated after Óladóttir *et al.*, 2008

*N1 and A1 have also been called T1 and T2 (Larsen *et al.*, 2005).

Silicic Katla eruptions during the last 8100 years

Published research about the Holocene silicic tephra from the Katla volcanic system is scant (e.g. Larsen *et al.*, 2001; Wastegård, 2002) and most research has focused on Katla's basaltic volcanism (e.g. Jakobsson, 1979; Thorarinsson, 1980; Larsen, 2000; Thordarson *et al.*, 2001; Óladóttir *et al.*, 2005, 2008). The best known silicic tephra from Katla, the wide-spread pre-Holocene Vedde Ash (e.g. Lacasse *et al.*, 1995; Wastegård *et al.*, 2000 a,b, Blockley *et al.*, 2007; Davies *et al.*, 2010) is outside the scope of this paper.

Of the 17 known silicic tephra layers, four have been dated by radiocarbon measurements on peat immediately below the tephra and 12 have been given an approximate age using soil accumulation rates (SAR) between tephra layers of known age (Table 1 and references therein). All are prehistoric. The most recent tephra layer, SILK-YN, is about 1620 years old (1676±12 ^{14}C BP).

The axes of thickness of six silicic layers intersect more or less inside the caldera (Figure 2). Although this points to a source of the silicic eruptions within the Katla caldera, it is also possible that the some occur at the caldera fracture (Larsen *et al.*, 2001). There are silicic rocks that outcrop along the caldera margin, e.g. at Austmannsbunga, but the geochemistry of the outcrops differs from that of the Holocene silicic tephra (Lacasse *et al.*, 2007).

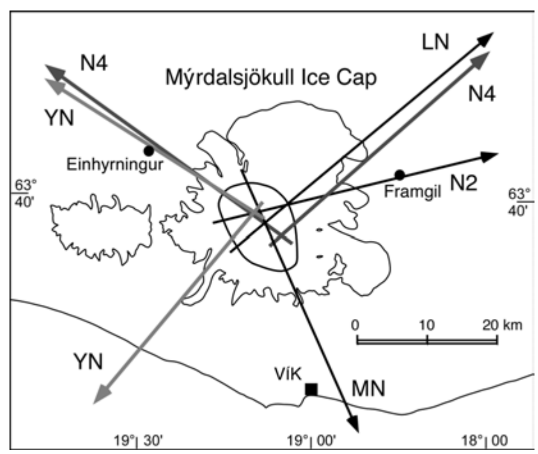

Figure 2. Axes of thickness of the silicic tephra layers from Katla and sampling locations (Larsen, 2000). – *Þykktarásar súrra gjóskulaga frá Kötlu og sýnatökustaðir (Larsen, 2000).*

Óladóttir *et al.* (2007) have shown that during the last 8400 years the sulphur degassing of the basaltic Katla tephra has been arrested, indicating that the basaltic Katla tephra was quenched by contact with water in hydromagmatic/phreatomagmatic eruptions. This indicates that the caldera was never ice-free during the last 8400 years, or at least there was water present. It is assumed that the silicic eruptions have been taking place under similar conditions as the basaltic Katla eruptions, under environmental conditions dominated by ice and meltwater.

Dispersal maps exist for six silicic tephra layers and the distribution and the shape of the tephra lobes of these silicic eruptions suggest that they were rather short-lived, with a relatively low eruption plume (Larsen *et al.*, 2001). Volume calculations of these six silicic tephra layers (Table 2) show that the silicic eruptions were generally smaller than known basaltic eruptions (Larsen *et al.*, 2001; Larsen, 2010, Óladóttir *et al.*, 2014). Silicic Katla tephra of Holocene age has nevertheless been found overseas, e.g. in the Faroe Islands and Ireland (Hall and Pilcher, 2002; Wastegård, 2002) and as ocean-transported pumice. e.g. on the coasts of Scotland, Norway and Svalbard (Newton 1999; Larsen *et al.*, 2001). These silicic Katla eruptions were classified as hydromagmatic by Larsen *et al.* (2001).

This silicic tephra from Katla volcano has specific characteristics in the field. Most of them are of olive-green to grey-green color and have elongated glass grains in varying amounts. Three of the 17 known silicic tephra layers have more distinctive characteristics. This difference lies both in the size and shape of the grains, as the grains are prominently needle shaped. The term „needle layer" was first used about these layers by Ólafsson *et al.* (1984), the prefix SILK (silicic Katla layer) was added later (Larsen, 2000). The needles form when vesicles are drawn out into tubes, often flattened, with very thin walls that break into needle-like grains or thin glass plates (Figure 3). The needle grains are very delicate and brittle because of these thin walls. The elongated grains have been measured up to more than 8 cm long and 1–2 cm wide. More equant grains, sometimes massive, occur as well in most of the layers. The needle layers have a very unusual appearance and are unique in Iceland, although there are some characteristic features in these layers, thin flat grains, that are similar to the tephra that was formed in the Öræfajökull eruption in 1362 (Larsen, 2000; Thorsteinsdóttir, 2012). It is worth mentioning that Dr. Grant Heiken, author of the Atlas

Table 2. Volumes of the youngest six SILK tephra layers on land. CPT stands for compacted tephra volume and UCP uncompacted or freshly fallen tephra (Larsen *et al.*, 2001). – *Rúmmál yngstu sex SILK gjóskulaganna (á landi). CPT er rúmmál á samþjappaðri gjósku og UCP rúmmál á ósamþjappaðri eða nýfallinni gjósku.*

SILK Tephra	CPT km^3	UCP km^3
Layer YN	0.04	0.08
Layer UN	0.16	0.27
Layer MN	0.03	0.05
Layer LN	0.12	0.20
Layer N4	0.07	0.11
Layer N2	0.04	0.06

Figure 3. Grains of silicic Katla (SILK) tephra. The largest grains are about 4 cm long. – *Korn súrrar Kötlu (SILK) gjósku (Ljósm./Photo. Guðrún Larsen).*

of Volcanic Ash (1974) and Volcanic Ash (1985) who kindly inspected a sample of the SILK-LN tephra in 2014, did not know of any other tephra having this characteristics (Heiken, personal comment, 2014).

Hydromagmatic/Phreatomagmatic eruptions

As many Icelandic volcanic systems are ice-covered, „wet eruptions“ are the most common type. Phreatomagmatic/hydromagmatic eruptions therefore characterize the volcanic activity in Iceland (e.g. Thordarson and Larsen, 2007; Thordarson and Höskuldsson, 2008), with basaltic eruptions the most frequent.

Hydromagmatic eruptions are divided into three categories: Phreatic eruptions where magma is not directly involved but provides the heat source, phreatomagmatic eruptions and phreatoplinian eruptions where the magma fragments as a result of interaction with water and becomes extremely fine grained tephra. Fragmentation processes in hydromagmatic eruptions are much more complex than in magmatic eruptions. The presence of external water can affect both fragmentation and cooling at various stages of an eruption.

Wohletz (1983) did a research on eruptive material formed by the interaction of magma and water. He designed a graph that shows maximum and minimum fragmentation caused by external water (Figure 4) which demonstrates the mass ratio of water and magma against efficiency and approximate median grain size. If the mass ratio of water/magma is less than 0.3, the efficiency decreases and the grains get bigger. In that kind of situation there are two things that maintain the explosive activity of the eruption; on the one hand volatiles and on the other hand steam. Once the mass ratio of water/magma is about 0.3, or even slightly higher, the magma-water interactions maintain the explosions in the eruption. At this stage, the efficiency is at its maximum, the fragmentation of magma is at its greatest and the smallest grains are produced (Cas and Wright, 1987; Wohletz, 1983).

Grains formed in phreatomagmatic basaltic eruptions have been classified into five main types and their formation has been clarified by experiments (e.g. Morrisey *et al.*, 2000; Wohletz, 1983). Blocky grains form by brittle fracture, when deformation rates exceed the tensile strength of the melt and also by thermal contraction in quenched portions of the melt. Fusiform grains with fluidal surfaces form from portions of melt that fragment prior to quenching. Moss-like grains form by viscous deformation under tensional stress conditions. Drop-like grains develop from the effect of surface tension from fluid melt. Plate-like grains are thought to be pieces stripped off quenched crust. One of the characteristics of phreatomagmatic basaltic eruptions is also the presence of lithics from substrata of the vents and from conduit walls.

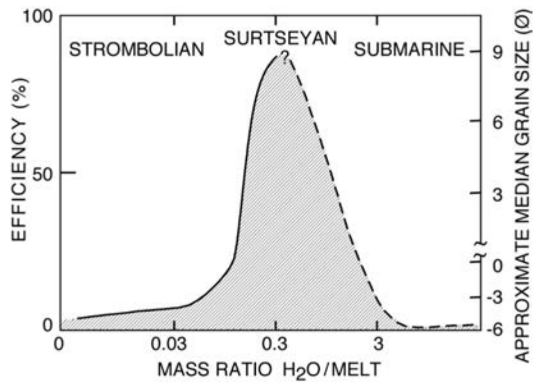

Figure 4. Mass ratio of water/magma versus efficiency and grain size (Wohletz, 1983). – *Massahlutfall vatns/kviku á móti afkastagetu og kornastærð.*

Phreatoplinian eruptions are less common compared to the other two types and not as well understood (White and Houghton, 2000; Morrisey *et al.*, 2000; Francis, 2001; Francis and Oppenheimer, 2004). This category was first recognized and named by Self and Sparks (1978), partly based on observations of the widespread unit C in the Askja 1875 eruption. The characteristics described by them were abundant fine ash, even near the source, well-bedded deposits and accretionary lapilli, all indicating the presence of water. Self and Sparks (1978) concluded that the extreme fragmentation was due to magma-water interaction superimposed on fragmentation caused by vesiculation and expansion of gases in the magma itself. The wide dispersal indicated deposition from a high eruption column. About 90% of the total grains size in Askja unit C was smaller than 1 mm (Sparks *et al.*, 1981).

Fragmentation in most of the phreatoplinian eruptions described by Houghton *et al.* (2000) was brought about by vesiculation and bubble expansion, as well as by quenching by external water. The pumice clasts were vesicular enough to imply that the magma had already formed foam and perhaps begun to fragment or disintegrate before it first encountered external water. The fragmentation resulting from the magma-water interaction could be the result of thermal contraction upon quenching, brittle failure caused by high strain rates resulting from expansion of steam or both these mechanisms. Lithics appear to be less common in phreatoplinian eruptions than in the basaltic ones. This could suggest that the fragmentation caused by water takes place at the interface between the magma and ice/water, rather than deeper in the conduit (Dellino *et al.*, 2012).

Knowledge about silicic phreatoplinian eruption columns or plumes is limited. It has been suggested that limited amount of water will have little effect on the height and dispersive power but excessive amount will cause column collapse and pyroclastic flows or surges (Houghton *et al.*, 2000).

Only two examples of recent subglacial explosive silicic (>63% SiO_2) eruptions were found in literature (Guðmundsson *et al.*, 2012; Kratzmann *et al.*, 2009). It is suggested that some phases of the 1991 Hudson eruption were phreatoplinian because of the fine ash produced. However, no phase of the Eyjafjallajökull eruption was classified as phreatoplinian, although about 94% of the tephra from the first phase (14-16 April) was smaller than 1 mm and up to 50% smaller than 0.063 mm (Gudmundsson *et al.*, 2012).

METHODS

Tephra samples were collected from soil sections at Framgil on Álftaversafréttur and Einhyrningur west of Markarfljót (Figure 2), 22 and 20 km from centre of caldera, respectively. At each location the tephra layers were cleaned, photographed, measured and macroscopic features described such as bedding, grading, colour, texture, grain size and grain types (for details see Thorsteinsdóttir 2015).

Grain analyses

Sieving by hand (to avoid breaking/abrading) was used for size fractions larger than 4Φ (0.063 mm) and settling velocity less than 4Φ. A Sedigraph (Micromeritics, 2010) was used for grains smaller than 4Φ. The results from both methods were combined and plotted on a graph, showing the complete grain size distribution of each tephra sample. The elongated grain shape of the SILK tephra may affect the size results because particle size techniques assume that grains are spherical. A comparison between the SILK tephra layers is however considered justified.

Grain morphology analysis was carried out on selected samples from four eruptions. The parameters ruggedness (ratio of convex perimeter to total perimeter, CPERIM/PERIM), elongation (ratio of minimum to maximum diameter, DMIN/DMAX) and circularity $(4\pi \text{AREA})/(\text{PERIM})^2$ were measured using an image analysis program (Eiríksson *et al.*, 1994).

Scanning electron microscope (SEM) images on selected tephra samples were obtained using a Hitachi TM3000 electron microscope, in order to demonstrate potential differences between tephra layers which might reflect different eruptive environments.

RESULTS

Samples from 10 SILK tephra layers were analysed for grain size and 4 samples for grain shape, including the previously analysed SILK-LN layer (Thorsteinsdóttir *et al.*, 2015). The main focus was on possible changes during the period from 2800 to 8100 years ago. The tephra samples were collected at similar distance, 20–22 km, from the center of Katla caldera. The thickness axes are, however, not known for all the layers. Tephra layers SILK-YN, SILK-MN and SILK-A9 were not included in this study. The remaining layers (except SILK-A11) were grain size analysed, and SILK-N1, SILK-A8, SILK-A11 and A12 were analysed for grain shape (Table 3).

Changes in grain size

The younger part of the silicic tephra sequence appears coarse grained while the older part is fine grained (Table 3). The largest grains in the coarser section belong to the grain size categories from -3Φ to

-1Φ whereas the largest grains from the finer grained section all except SILK-A7 belong to grain size category 0 Φ. The „change“ in grain size occurs between 5800 and 6000 years ago. The mean grain size, however, is more variable. The majority of tephra layers younger than 5000 years have mean grain size of 2.2 to 1.1 Φ (0.2 to 0.45 mm) whereas the majority of SILK layers older than 5000 years have mean grain size of ∼3 to ∼4 Φ, or smaller than 0.125 mm. Examples are shown in Figure 5.

Table 3. Grain size$^{\triangle}$ and grain shape* analyzes of 12 SILK tephra layers. Age and associated references are in Table 1. – *Listi yfir 12 SILK gjóskulög sem voru kornastærðar$^{\triangle}$- og kornalögunar*greind. Upplýsingar um aldur gjóskulaganna og heimildir eru í töflu 1.*

Tephra layer	Rounded age	Largest Φ	Mean Φ
SILK-UN$^{\triangle}$	∼2800	-3	1.62
SILK-LN$^{\triangle}$*	∼3400	-3	2.24
SILK-N4$^{\triangle}$	∼3900	-1	3.96
SILK-N3$^{\triangle}$	∼4100	-3	1.12
SILK-N2$^{\triangle}$	∼5000	-1	2.01
SILK-N1$^{\triangle}$*	∼5800	-1	3.03
SILK-A1$^{\triangle}$	∼6000	0	3.52
SILK-A5$^{\triangle}$	∼7100	0	3.47
SILK-A7$^{\triangle}$	∼7200	-2	1.61
SILK-A8$^{\triangle}$*	∼7400	0	3.88
SILK-A11*	∼8000	–	–
SILK-A12$^{\triangle}$*	∼8100	0	2.96

Changes in grain shape

Grain shape analyses were performed on the SILK-N1, SILK-A8, SILK-A11 and SILK-A12 tephra layers, sampled at about 20 km distance from source at Einhyrningsflatir and SILK-LN (Thorsteinsdóttir *et al.*, 2015) sampled at Geldingasker about 33 km from source (Table 4). SILK-A11 is significantly different from the other layers with an elongation value of 0.78 (value of 1 is a perfect circle). SILK-A11 grains are slightly less elongated than those from the Hekla-1947 tephra layer (0.73) which was erupted subaerially. All other SILK layers have elongation values between 0.52 and 0.69 and more elongated grains. No systematic change is observed with time, the grains are most elongated in the oldest A12 layer with a value of 0.52 and least elongated in the second oldest A11 layer (0.78). Within the bedded layers SILK-N1 and SILK-LN the values change towards less elongated grains with time (Table 4).

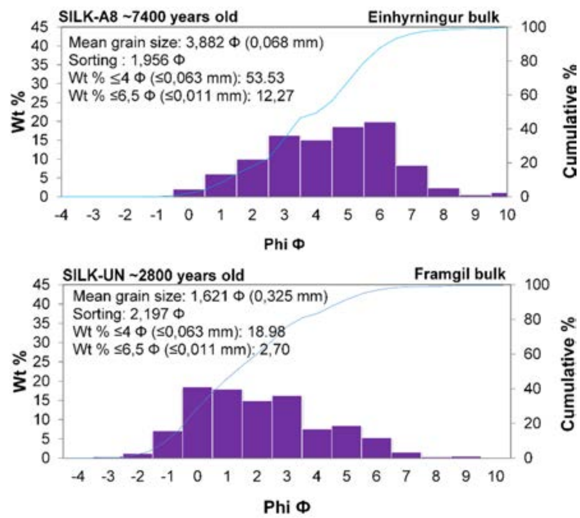

Figure 5. Grain size distribution of two SILK layers. A) SILK-A8 fine grained and B) SILK-UN coarser grained. – *Kornastærðardreifing (Φ) tveggja SILK laga. SILK-A8 er fínkornóttara og SILK-UN grófkornóttara.*

Table 4. Results of grain shape measurements, elongation (lower values represent more elongated grains), ruggedness (R2) (lower values represent more rugged grains) and circularity (higher values for more circular grains). – *Niðurstöður kornalögunargreininga á ílengd (lægra gildi – ílengri korn), hrjúfleika (lægri gildi – hrjúfara korn) og hringlögun (hærra gildi – kringlóttara korn).*

Layer/Unit	Elong.	R2	Circ.	Age
SILK-LN middle unit	0.68	0.33	0.67	3400
SILK-LN bottom unit	0.55	0.36	0.63	3400
SILK-N1 middle unit	0.69	0.41	0.73	5800
SILK-N1 bottom unit	0.58	0.40	0.66	5800
SILK-N1 average	0.64	0.40	0.70	5800
SILK-A8	0.69	0.42	0.74	∼7400
SILK-A11	0.78	0.35	0.78	∼8000
SILK-A12	0.52	0.42	0.65	∼8100

The ruggedness values are all quite similar except for SILK-A11, and if SILK-A11 is excluded, the ruggedness increases slightly with time (the ruggedness values get lower). The ruggedness value for SILK-A11 is 0.35, so the grains in SILK-A11 have more uneven outlines than in the other three layers. The difference between A12, A8 and N1 is small, from 0.42 in the oldest layer to average of 0.40 in the youngest layer. The values of the N1 layer do not change very much internally or from 0.40 in the bottom unit to 0.41 in the middle unit. No systematic change in ruggedness with time is seen even though SILK-LN is included and SILK-A11 omitted.

The circularity value in the oldest layer A12 is among the lowest measured but it increases significantly in the A11 layer as observed in both elongation and ruggedness. Then the values slowly trend away from circular shape. The values for SILK-A8 and SILK-N1 (average) are 0.74 and 0.70, respectively. Within bedded layer circularity increases with time, the value in the bottom unit is 0.66 and 0.73 in the middle layer. Overall there is no systematic change in circularity with time in the tephra layers investigated even though SILK-LN is included and SILK-A11 omitted.

In summary, the SILK-A11 tephra layer is very different from the other three SILK layers in all parameters measured. The grains are not elongated but rather circular in shape and have more uneven surface. The other grains from the SILK layers including the SILK-LN layer have much more elongated shape, less circularity and smoother surface. This difference is demonstrated in Figure 6. During the period investigated (between ∼3400 and ∼8100 years ago) no systematic changes with time were seen in the grain parameters of the SILK layers.

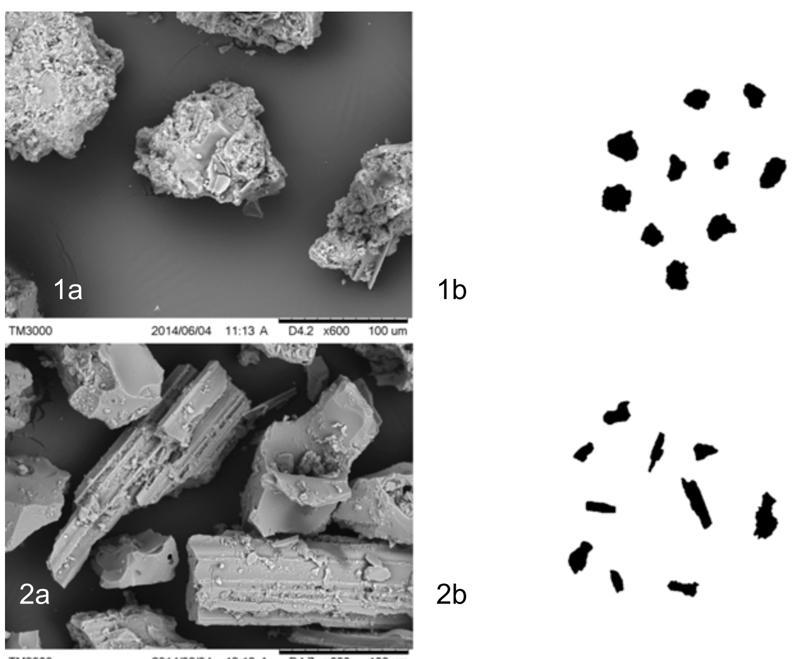

Figure 6. SEM (TM3000) and shadow (Morphocop) images showing differences between the two oldest SILK tephra layers, A11 and A12. 1a: SEM image from SILK-A11. 1b: Shadow image from SILK-A11. 2a: SEM image from SILK-A12. 2b: shadow image from SILK-A12. – *SEM myndir (TM3000) og skuggamyndir (Morphocop) sem sýna muninn á milli tveggja elstu SILK gjóskulaganna A12 og A11. SEM mynd (1a) og skuggamynd (1b) af SILK-A11. SEM mynd (2a) og skuggamynd (1b) af SILK-A12.*

Changes in chemical composition with time

Thirteen silicic tephra layers from Katla volcano have been chemically analyzed or the majority of the silicic tephra layers. The average values of the major element composition of the SILK layers YN, UN, MN, LN, N4, N3, N2, N1, A1, A8, A9 (Larsen *et al.*, 2001) A11 and A12 (Newton, 1999 and previously unpublished analyses) are shown in Table 5.

The chemical composition of the tephra from the SILK layers reveals discrete changes between individual layers, as indicated by colors and arrows in Table 5. The compositional changes of SILK-YN, -UN, -MN, -LN, -N4, -N3, -N2, -N1, -A1, -A8 and -A9 have been treated by Larsen *et al.* (2001) where two groups are apparent (Figure 7). SILK-UN, SILK-N3, SILK-N2 and SILK-A8 tephra layers have somewhat lower SiO_2, higher MgO and CaO and generally higher TiO_2 than SILK-YN, SILK-MN, SILK-LN, SILK-N4, SILK-N1, SILK-A1 and SILK-A9.

TiO_2, MgO and CaO abundances are considerably lower and SiO_2 is higher in the two oldest tephra layers, SILK-A11 and SILK-A12, than in all the other SILK layers (Table 5). This difference between the tephra layers is presented in Figure 7, where CaO is plotted against FeO. The two oldest tephra layers form the third group on the plot. Tephra samples analyzed for grain size and grain shape characteristics came from the three „groups“ (see Table 3).

There appears to be potential correlation between grain sizes and chemical composition of the 11 SILK tephra layers analyzed for grain size (Tables 3 and 5). When considering the largest Φ (Table 3) the tephra layers with lower SiO_2 and higher MgO, CaO and TiO_2 tend to be coarser grained than the others. Although samples from only five SILK tephra layers have been analyzed for grain shape so far, there seems to be no correlation between chemical composition and the grain shape parameters. This is best demonstrated by very significant difference in grain shape parameters between SILK-A11 and -A12 (Table 4), although their chemical composition is very similar (Figure 6).

Table 5. Average chemical analyses (wt %) performed on the SILK layers YN, UN, MN, LN, N4, N3, N2, N1, A1, A8 and A9. Layers UN, N3, N2 and A8 show higher TiO_2 , MgO and CaO and lower SiO_2 concentration than the other 8 layers (red colored numbers). A11 and A12 show higher SiO_2 and lower TiO_2 , MgO and CaO abundances compare to the other 11 layers (purple colored numbers) (Newton, 1999; Larsen *et al.*, 2001 and unpublished data). Grain size$^{\triangle}$ and grain shape* analysed material. – *Meðaltalsgildi (wt%) efnagreininga á SILK lögunum YN, UN, MN, LN, N4, N3, N2, N1, A1, A8 og A9. UN, N3, N2 og A8 hafa hærra hlutfall TiO_2, MgO og CaO og lægra hlutfall SiO_2 en hin átta lögin (rauðar tölur). A11 og A12 hafa hærra hlutfall SiO_2 og lægra hlutfall TiO_2 , MgO og CaO en hin 11 lögin (fjólubláar tölur) (Newton, 1991; Larsen og fl., 2001 og óútgefin gögn). Kornastærðar$^{\triangle}$ og kornalögunar* greint efni.*

Tephra	SiO_2	TiO_2	Al_2O_3	FeO	MnO	MgO	CaO	Na_2O	K_2O	Total
SILK-YN	65,31	1,19	14,15	6,04	0,19	1,06	2,94	4,55	2,70	98,12
SILK-UN$^{\Delta}$	64,16↓	1,33↑	13,95	5,94	0,20	1,36↑	3,40↑	4,37	2,59	97,30
SILK-MN	65,39	1,19	14,21	5,54	0,21	1,13	2,96	4,22	2,63	97,48
SILK-LN$^{\Delta*}$	65,23	1,21	14,25	5,62	0,19	1,12	3,02	4,42	2,76	97,84
SILK-N4$^{\Delta}$	66,19	1,23	14,10	5,57	1,79	1,14	2,90	4,50	2,80	98,61
SILK-N3$^{\Delta}$	64,69↓	1,48↑	14,15	5,96	2,02	1,35↑	3,35↑	4,25	2,60	98,02
SILK-N2$^{\Delta}$	63,59↓	1,52↑	13,94	6,35	0,21	1,44↑	3,60↑	4,32	2,53	97,49
SILK-N1$^{\Delta*}$	65,34	1,37	13,67	5,78	0,19	1,19	3,03	4,52	2,78	97,83
SILK-A1$^{\Delta}$	65,83	1,21	14,15	5,52	0,18	1,15	3,07	4,41	2,80	98,22
SILK-A8$^{\Delta*}$	64,44↓	1,25↑	14,00	5,78	0,17	1,23↑	3,34↑	4,61	2,65	97,46
SILK-A9	64,88	1,14	14,00	5,45	0,14	1,14	3,10	4,60	2,70	97,17
SILK-A11*	68,59	0,88	13,86	4,26	0,17	0,74	2,09	4,41	3,13	98,38
SILK-A12$^{\Delta*}$	69,07	0,85	13,98	4,21	0,15	0,80	2,07	5,03	3,10	99,40

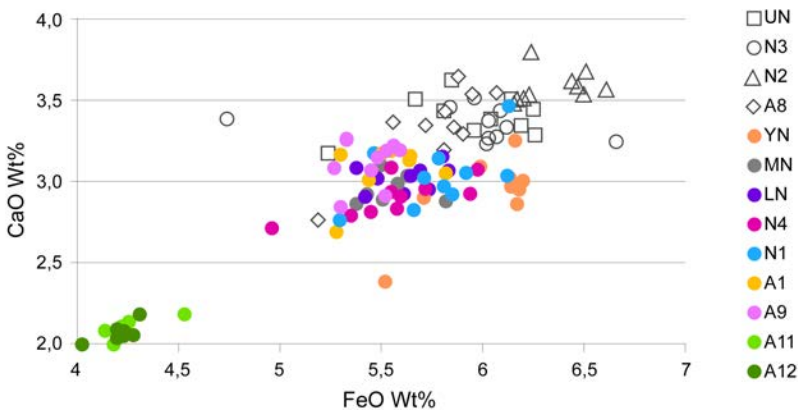

Figure 7. Graph that shows CaO wt% values plotted against FeO wt%. The SILK-UN, N3, N2 and A8 have higher values in CaO than the other 9 layers (Larsen *et al.*, 2001). – *Meðaltalsgildi (wt%) CaO á móti FeO (Larsen o. fl., 2001).*

DISCUSSION: CHANGES THROUGH THE HOLOCENE

The main changes in the grain size of the 12 Holocene SILK layers (2800 and 8100 years ago) from the Katla volcano are that the younger layers (2800–5800 year old) appear to be coarser grained than the older ones (6000–8100 year old). An exception is the SILK-A7 which is coarser grained than the other older layers.

The factors that could cause differences in grain size and grain morphology are 1) external factors, in particular the presence and availability of meltwater and 2) internal factors, such as changing composition of the magma and the volume erupted.

Tephra produced in phreatomagmatic eruptions is often characterized by being highly fragmented. The ratio of water to magma affects the explosive activity and fragmentation of the magma (e.g. Wohlets, 1983; White and Houghton, 2000; Morrisey *et al.*, 2000; Francis, 2001; Francis and Oppenheimer, 2004) and for this reason reduced fragmentation of erupting magma and consequently coarser grained tephra in a sub-glacial environment, could be the result of thinner ice cover and therefore less available meltwater.

A general trend towards coarser-grained tephra in the younger SILK layers is shown by the data in Table 3. This could suggest a thinner ice cover 2800-5800 years ago compared to when the older SILK layers were forming. This is supported by the end-moraines of Sólheimajökull which suggest a receding ice cap since at least 4500 years ago, and the outermost moraine could be as much as 7000 years old (Dugmore, 1989). The two largest SILK layers are amongst the coarser grained younger layers, so the duration of an eruption could also be important, with longer eruptions creating a less wet environment due to a reduction in the amount of ice in contact with the magma over time. The location of eruption sites may also have changed within the caldera to an area of thinner ice. It should also be kept in mind that not all tephra samples came from axes of greatest thickness which could affect the result.

Grain shape analyses revealed that the SILK-A11 tephra layer is dissimilar to the other analyzed SILK tephra layers. Firstly, SILK-A11 grains are less elongated and this is supported by the circularity value of A11 indicating that they are closer to being circular in shape compared to the more elongated grains of the other SILK layers. SILK-A11 grains also have much rougher surfaces than those from the other layers. The reasons why this particular layer is so different from the other SILK layers are not obvious. Perhaps there was less water present than in the other eruptions or maybe the chemical composition of the SILK-A11 tephra layer is important. Chemical analysis of the SILK-A11 reveals that it differs from nearly all the other SILK layers, but is very similar to SILK-A12. However, as SILK-A12 has the typical elongated grains found in the other SILK tephra layers, geochemical composition seems an unlikely reason for SILK-A11's differences. The small age difference between SILK-A11 and SILK-A12 eruptions (∼100 years) makes major changes in the glacier thickness unlikely. A different source area with different ice thickness and meltwater supply at the vents is a more likely explanation.

Dellino and Volpe (1996) analyzed grain shapes with the purpose of identifying the origin of the grains, in order to establish if they were of hydromagmatic or magmatic origin. Their work suggested that spherical shaped grains originate from hydromagmatic eruptions. However, Eiríksson and Wigum (1989) state that grains from silicic magmas are more readily elongated than those from basaltic ones and magmatic grains tend to be more elongated than the hydromagmatic grains. According to the elongation values, the SILK grains are very elongated, which agrees with Eiríksson and Wigum (1989). The high proportion of fine grained material also supports phreatomagmatic activity (Self and Sparks, 1978).

We believe that the elongated SILK grain shape is connected to phreatomagmatic explosive activity. The extreme elongate shape is the result of the break-up of viscous silicic magma with abundant elongate vesicles, as a result of a shock caused either by cooling contraction, a sudden expansion of steam, or both. In the case of the SILK-A11 tephra, the fragmentation occurred before the vesicles acquired an elongated form. We speculate that the ice at the eruption site was thicker and degassing was arrested by abundant meltwater before the magma froth was drawn out into the elongated vesicles that characterize other SILK-type tephras from this period.

SUMMARY

The younger SILK tephra layers appear to be coarser grained, i.e. have larger maximum grain size, while the older layers appear to be finer grained, except for SILK-A7. These changes occur between SILK-N1 (∼5800 year old) and SILK-A1 (∼6000 year old). However, the mean grain size does not clearly follow this trend.

Grain shape results for the SILK-LN, SILK-N1, SILK-A8, SILK-A11 and SILK-A12 tephra layers show that SILK-A11 is significantly different from the other four layers. The main difference lies in the elongation values, as no systematic changes with time were observed in the shape parameters (elongation, ruggedness and circularity). Omitting SILK-A11 and adding the ∼3400 old SILK-LN to the measurements does not change this conclusion.

The chemical composition of the SILK-A11 and SILK-A12 show higher SiO_2 values and lower TiO_2, MgO and CaO values compared to all other SILK layers.

Grain size and chemical composition appear to be correlated, where the SILK tephra layers with the lowest SiO_2 and highest FeO and CaO tend to be coarser grained than the others, but there is no correlation between grain shape (parameters measured in this study) and chemical composition.

The results of this study do not support radical changes in the eruption environment. On the contrary, the results support a fairly stable eruption conditions during the period under investigation, and presence of ice cover throughout the Holocene as suggested by Dugmore (1989) and Óladóttir *et al.* (2007).

Acknowledgements

This work was supported by the International Civil Aviation Organization (ICAO) as a part of the Catalogue of Icelandic Volcanoes Project of the Icelandic Meteorological Office and the Institute of Earth Sciences, University of Iceland. We are grateful to Bergrún A. Óladóttir, Johanne Schmith, Tinna Jónsdóttir and Agnes Ö. Magnúsdóttir for assistance and good company in the field, and to Jón Eiríksson for assistance with the grain shape analyses. We thank the two reviewers for their constructive reviews.

ÁGRIP

Kornastærð og kornalögun súrrar til ísúrrar gjósku úr 12 Kötlugosum, sem urðu fyrir 2800 til 8100 árum, var rannsökuð með það að markmiði að kanna hvort kornaeinkenni gjóskunnar hefðu breyst með tíma og í slíku tilfelli hvort breytingarnar endurspegluðu breytingar á umhverfi gosstöðvanna eða einhverjar aðrar ástæður, t.d. breytta efnasamsetningu. Kornastærðargreiningarnar benda til að gjóska í yngri gosunum sé yfirleitt heldur grófari en í þeim eldri, þó með ákveðnum undantekningum. Þessi „breyting" í átt að heldur grófari gjósku átti sér stað fyrir 5800–6000 árum.

Engar kerfisbundnar breytingar fundust á kornalögun súru/ísúru Kötlugjóskunnar með tíma. Þær breytur sem mældar voru eru ílengd, hrjúfleiki og hringlögun. Gjóskan einkennist af ílöngum (oft nálarlaga) kornum með útdregnum gasblöðrum - að undanskildri gjósku úr næstelsta gosinu sem skar sig úr öllum hinum með hringlaga kornum og óreglulegum gasblöðrum. Skipta má gjóskulögunum í 3 hópa samkvæmt efnasamsetningu gjóskunnar. Elstu gjóskulögin tvö mynda einn hópinn en í hinum tveim tengist breytileikinn ekki aldri eða tíma.

Þykkari jökull og meira bræðsluvatn fyrir 6000–8100 árum gæti orsakað hærra hlutfall fínnar gjósku í flestum eldri gosanna. Grófari gjóska í yngri lögunum gæti þannig hafa myndast við gos undir þynnri jökli eða færslu á gosstöðvum til svæða með þynnri ís. Í tilfelli stærstu gjóskulaganna gæti aðgangur að vatni hafa minnkað í löngum gosum. Ekki er hægt að draga þá ályktun af kornaeinkennum gjóskunnar að meiriháttar breytingar hafi orðið á umhverfi gosstöðvanna heldur benda þær til að aðstæður hafi verið fremur stöðugar á tímabilinu sem rannsakað var. Stór jökulhlaup (allt að 200 þúsund m^3 s^{-1}) á þessu tímabili styðja einnig að gosstöðvarnar hafi verið undir jökli.

REFERENCES

Björnsson, H. 2008. *Jöklar á Íslandi.* Opna, Reykjavík, 479 pp.

Björnsson, H., F. Pálsson and M. T. Guðmundsson 2000. Surface and bedrock topography of the Mýrdalsjökull ice cap, Iceland: The Katla caldera, eruption sites and routes of jökulhlaups. *Jökull* 49, 29–46.

Blockley, S. P. E., C. S. Lane, A. F. Lotter and A. M. Pollard 2007. Evidence for the presence of the Vedde Ash in Central Europe. *Quat. Sci. Rev.* 26, 3030–3036.

Bonadonna, C. and B. F. Houghton 2005. Total grain-size distribution and volume of tephra-fall deposits. *Bull. Volcanol.* 67, 441–456.

Büttner, R., P. Dellino, L. La Volpe, V. Lorenz and B. Zimanowski 2002. Thermohydraulic explosions in phreatomagmatic eruptions as evidenced by the comparison between pyroclasts and products from Molten Fuel Coolant Interaction experiments. *J. Geophys. Res.* 107, ECV 5-1-ECV 5–14. doi:10.1029/2001JB000511.

Cas, R. A. F. and J. V. Wright 1987. *Volcanic Successions, Modern and Ancient.* London: Allen and Unwin, 528 pp.

Cioni, R., M. Pistolesi, A. Bertagnini, C. Bonadonna, A. Höskuldsson and B. Scateni 2014. Insights into the dynamics and evolution of the 2010 Eyjafjallajökull summit eruption (Iceland) provided by volcanic ash textures. *Earth Planet. Sci. Lett.* 394, 111–123.

Davies, S. M., G. Larsen, S. Wastegård, C. S. M. Turney, V. A. Hall, L. Coyle and T. Thordarson 2010. Widespread dispersal of Icelandic tephra: how does the Eyjafjöll eruption of 2010 compare to past Icelandic events? *J. Quat. Sci.* 25, 605–611. ISSN 0267–8179.

Dellino, P. and L. La Volpe, 1995. Fragmentation versus transportation mechanisms in the pyroclastic sequence of Monte Pilato-Rocche Rosse (Lipari, Italy). *J. Volcanol. Geotherm. Res.* 64, 211–231.

Dellino, P. and L. La Volpe, 1996. Image processing analysis in reconstructing fragmentation and transportation mechanisms of pyroclastic deposits. The case of Monte Pilato-Rocche Rosse eruptions, Lipari (Aeolian Islands, Italy). *J. Volcanol. Geotherm. Res.* 71, 13–29.

Dellino, P. and G. Liotino 2002. The fractal and multifractal dimension of volcanic ash particles contour: a test study on the utility and volcanological relevance. *J. Volcanol. Geotherm. Res.* 113, 1–18.

Dellino, P., M. T. Gudmundsson, G. Larsen, D. Mele, J. A. Stevenson, T. Thordarson and B. Zimanowski 2012. Ash from the Eyjafjallajökull eruption (Iceland): Fragmentation processes and aerodynamic behavior. *J. Geophys. Res.* 117, B00C04, 10 pp. doi:10.1029/2011JB008726.

Dugmore, A. J. 1989. Tephrochronological studies of Holocene glacier fluctuations in South Iceland. In: Oerlemans, J. (ed), *Glacier Fluctuations and Climate Change.* Kluwer Academic, Dordrecht, 37–55

Eggertsson, Ó. 2013. Ný aldursákvörðun fornskógar. Skógrækt Ríkisins, http://www.skogur.is/um-skograekt-rikisins/frettir/nr/1906.

Eiríksson, J. and B. J. Wigum 1989. The morphometry of selected tephra samples from Icelandic volcanoes. *Jökull* 39, 57–74.

Eiríksson, J., M. Á. Sigurgeirsson and T. Hoelstad 1994. Image analysis and morphometry of hydromagmatic and magmatic tephra grains, Reykjanes volcanic system, Iceland. *Jökull* 44, 41–55.

Flowers, G. E., H. Björnsson, Á. Geirsdóttir, G. H. Miller, J. L. Black, G. K. C. Clarke 2008. Holocene climate conditions and glacier variation in central Iceland from physical modelling and empirical evidence. *Quat. Sci. Rev.* 27, 798–813.

Francis, P. 2001. *Volcanoes A Planetary Perspective.* Oxford: Clarendon Press, 443 pp.

Francis, P. and C. Oppenheimer 2004. *Volcanoes.* New York: Oxford University Press Inc., 521 pp.

Gröndal, G. O., G. Larsen and S. Elefsen 2005. Stærðir forsögulegra hamfaraflóða í Markarfljóti – mæling á farvegum neðan Einhyrningsflata. (Magnitudes of prehistoric catastrophic floods in the Markarfljót river – survey of flood channels south of Einhyrningsflatir.) In: Guðmundsson, M. T. and Á G. Gylfason (eds.). *Hættumat vegna eldgosa og hlaupa frá vestanverðum Mýrdalsjökli og Eyjafjallajökli.* The National Commissioner of the Icelandic Police and the University Press, Reykjavík, 99–104.

Guðmundsdóttir, E. R. 1998. *Gjóska úr Kötlugosi 1755. Ásýnd, kornastærð og kornalögun.* B.Sc. Thesis, Univ. Iceland, Reykjavík, 64 pp.

Guðmundsson, M. T., T. Thordarson, Á. Höskuldsson, G. Larsen, H. Björnsson, F. J. Prata, B. Oddson, E. Magnússon, Th. Högnadóttir, G. N. Petersen, C. L. Hayward, J. A. Stevenson and I. Jónsdóttir 2012. Ash generation and distribution from the April-May 2010 eruption of Eyjafjallajokull, Iceland. *Scientific reports* 2 (572), 12 pp.

Hall, V. A. and J. R. Pilcher 2002. Late-Quaternary Icelandic tephras in Ireland and Great Britain: detection, characterization and usefulness. *The Holocene* 12, 223–230.

Heiken, G. 1974. An Atlas of Volcanic Ash. *Smithsonian Contr. Earth Sci.* 12.

Heiken, G. and K. Wohletz1985. *Volcanic Ash.* Berkeley, University of California Press, 246 pp.

Houghton, B., C. Wilson, R. Smith and J. Gilbert 2000. Phreatoplinian eruptions. In: H. Sigurdsson, B. Houghton, S. R. McNutt, H. Rymer, J. Stix (eds), *Encyclopedia of Volcanoes.* Academic Press, San Diego, 513–525.

Jakobsson, S. P. 1979. Petrology of recent basalts of the Eastern Volcanic Zone, Iceland. *Acta Naturalia Isl.* 26, 1–103.

Kratzmann, D. J., S. Carey, R. Scasso, and J. A. Naranjo 2009. Compositional variations and magma mixing in the 1991 eruptions of Hudson volcano, Chile. *Bull. Volcanol.* 71, 419–439.

Lacasse, C., H. Sigurdsson, H. Jóhannesson, M. Paterne, and S. N., Carey, L. E. 1995. Source of Ash Zone 1 in the North Atlantic. *Bull. Volcanol.* 57, 18–32.

Lacasse, C., H. Sigurdsson, S. N. Carey, H. Jóhannesson, L. E. Thomas and N. W. Rogers, 2007. Bimodal volcanism at the Katla subglacial caldera, Iceland: insight into the geochemistry and petrogenesis of rhyolitic magmas. *Bull. Volcanol.* 69, 373–399.

Larsen, G. 2000. Holocene eruptions within the Katla volcanic system, south Iceland: Characteristics and environmental impact. *Jökull* 49, 1–28.

Larsen, G., A. J. Newton, A. J. Dugmore and E. G. Vilmundardóttir 2001. Geochemistry, dispersal, volumes and chronology of Holocene silicic tephra layers from the Katla volcanic system, Iceland. *J. Quat. Sci.* 16, 119–132.

Larsen, G., K. Smith, A. Newton and Ó. Knudsen 2005. Jökulhlaup til vesturs frá Mýrdalsjökli: Ummerki um forsöguleg hlaup niður Markarfljót. (Volcanogenic floods towards west from Mýrdalsjökull ice cap: indications of prehistoric floods in the Markarfljót river.) In: Magnús T. Guðmundsson og Ágúst G. Gylfason (eds.): *Hættumat vegna eldgosa og hlaupa frá vestanverðum Mýrdalsjökli og Eyjafjallajökli.* The National Commissioner of the Icelandic Police and the University Press, Reykjavík, 75–98.

Larsen, G. 2010. Katla: Tephrochronology and eruption history. *Developm. Quat. Sci.* 13, 23–49.

Maizels, J. 1994. The origin and evolution of Holocene sandur deposits in areas of jökulhlaup drainage, Iceland. In: Maizels, J. K. and C. Caseldine, (eds.). *Environmental change in Iceland: past and present.* Kluwer Academic Publishers, Dordrecht, 267–302.

Micromeritics 2010. *SediGraph III 5120, Operator's Manual* (V1.04). Norcross, GA.

Morrisey, M., B. Zimanowski, K. Wohletz and R. Büttner 2000. Phreatomagmatic fragmentation. In: Sigurðsson, H., B. Houghton, S. R. Mcnutt, H. Rymer, and J. Stix (eds.), *Encyclopedia of Volcanoes.* San Diego, Academic Press. 431–445.

Newton, A. 1999. *Ocean transported pumice in the North Atlantic.* PhD thesis, Univ. Edinburgh, 394 pp.

Óladóttir, B. A. 2003. *Gjóskulagið E2 úr Kötlu; kornalögun og kornastærð.* B.Sc. Thesis, Univ. Iceland, Reykjavík, 90 pp.

Óladóttir, B. A., G. Larsen, Þ. Þórðarson and O. Sigmarsson 2005. The Katla volcano S-Iceland: Holocene tephra stratigraphy and eruption frequency. *Jökull* 55, 53–74.

Óladóttir, B. A., Th. Thordarson, G. Larsen and O. Sigmarsson 2007. Survival of the Mýrdalsjökull ice cap through the Holocene thermal maximum: evidence from sulphur contents in Katla tephra layers (Iceland) from the last ∼8400 years. *Ann. Glaciol.* 45, 183–188.

Óladóttir, B. A., O. Sigmarsson, G. Larsen and Th. Thordarson 2008. Katla volcano, Iceland: magma composition, dynamics and eruption frequency as recorded by Holocene tephra layers. *Bull. Volcanol.* 70, 475–493.

Óladóttir B. A., G. Larsen and O. Sigmarsson 2014. Volume estimates of nine prehistoric (∼1860 BC – 870 AD) Katla tephra layers. *Jökull* 64, 23–42.

Ólafsson, M., P. Imsland and G. Larsen 1984. Nornahár II (Pelé's hair II). *Náttúrufræðingurinn* 53, 135–144.

Rose, W. I. and A. J. Durant 2009. Fine ash content of explosive eruptions. *J. Volcanol. Geotherm. Res.* 186, 32–39.

Self, S. and R. S. J. Sparks 1978. Characteristics of widespread pyroclastic deposits formed by the interaction of silicic magma and water. *Bull. Volcanol.* 41 (3), 196–212.

Smith, K. T. and A. J. Dugmore 2006. Jökulhlaups circa landnám: mid- to late first millennium AD floods in south Iceland and their implications for landscapes of settlement. *Geografiske Ann.* 88A, (2), 165–176.

Sparks, R. S. J., L. Wilson and H. Sigurdsson 1981. The pyroclastic deposits of the 1875 eruption of Askja, Iceland. *Phil. Trans. Royal Soc. London*, series A 299, 241–273.

Thorarinsson, S. 1980. Langleiðir gjósku úr þremur Kötlugosum. *Jökull* 30, 65–73.

Thordarson, T. and G. Larsen 2007. Volcanism in Iceland in historical time: Volcano types, eruption styles and eruptive history. *J. Geodyn.* 43, 118–152.

Thordarson, Th. and Á. Höskuldsson 2008. Postglacial volcanism in Iceland. *Jökull* 58, 197–228.

Thordarson, T., D. J. Miller, G. Larsen, S. Self and H. Sigurdsson 2001. New estimates of sulfur degassing and atmospheric mass-loading by the 934 AD Eldgjá eruption, Iceland. *J. Volcanol. Geotherm. Res.* 1108, 33–54.

Thorsteinsdóttir, E.. S. 2012. *Súr gjóska úr Kötlu. Kornastærð, kornalögun og þáttagreining.* B.Sc. Thesis, Univ. Iceland, Reykjavík, 54 pp.

Thorsteinsdóttir, E. S. 2015. *Grain characteristics of tephra from the subglacial SILK-LN Katla eruption ∼3400 years ago and the subaerial Hekla eruption in 1947.* M.Sc. Thesis, Univ. Iceland, Reykjavík, 165 pp.

Thorsteinsdóttir, E. S., E. R. Gudmundsdóttir and G. Larsen 2015. Grain characteristics of tephra from the subglacial SILK-LN Katla eruption ∼3400 years ago and the sub-aerial Hekla eruption in 1947. *Jökull* 65, 29–49.

Wastegård, S. 2002. Early to middle Holocene silicic tephra horizons from the Katla volcanic system, Iceland: new results from the Faroe Islands. *J. Quat. Sci.* 17, 723–730.

Wastegård, S., C. S. M. Turney, J. J. Lowe and S. J. Roberts 2000a. New discoveries of the Vedde Ash in southern Sweden and Scotland. *Boreas* 29, 72–78.

Wastegård, S., B. Wohlfarth, D. A. Subetto and T. V. Sapelko 2000b. Extending the known distribution of the Younger Dryas Vedde Ash into northwestern Russia. *J. Quat. Sci.* 15, 581–586.

White, J. D. and B. Houghton 2000. Surtseyjan and related phreatomagmatic eruptions. In: Sigurðsson, H., B. Houghton, S. R. Mcnutt, H. Rymer and J. Stix (eds.), *Encyclopedia of Volcanoes*, Academic Press, San Diego, 495–411.

Wohletz, K. H. 1983. Mechanisms of hydrovolcanic pyroclast formation: grain-size, scanning electron microscopy, and experimental studies. *J. Volc. Geotherm. Res.* 17, 31–63.